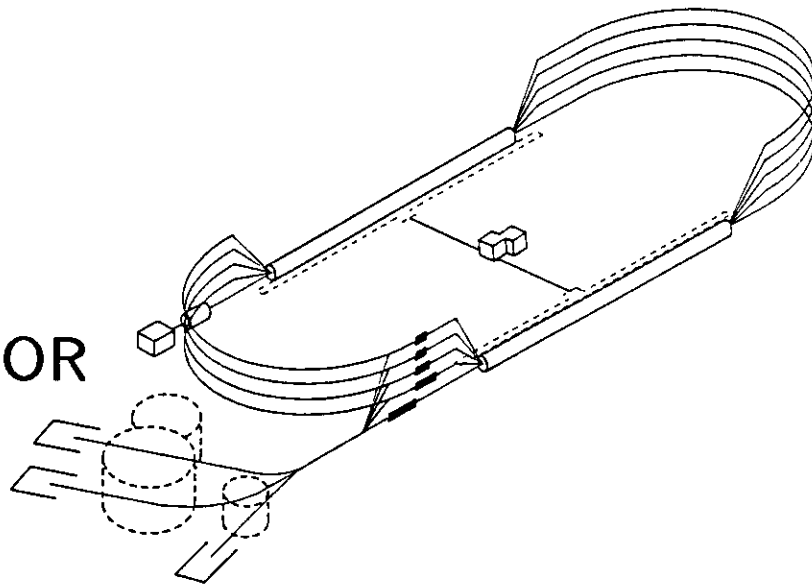


Polarization Phenomena in Electromagnetic Interactions  
at Intermediate Energies

Volker Burkert  
Continuous Electron Beam Accelerator Facility  
Newport News, VA 23606

Invited talk presented at the 7<sup>th</sup> International Conference on  
Polarisation Phenomena in Nuclear Physics, Paris, July 9 - 13, 1990.

**C**ONTINUOUS  
**E**LECTRON  
**B**EAM  
**A**CCCELERATOR  
**F**ACILITY



**SURA** SOUTHEASTERN UNIVERSITIES RESEARCH ASSOCIATION

**CEBAF**

**Newport News, Virginia**

Copies available from:

Library  
CEBAF  
12000 Jefferson Avenue  
Newport News  
Virginia 23606

The Southeastern Universities Research Association (SURA) operates the Continuous Electron Beam Accelerator Facility for the United States Department of Energy under contract DE-AC05-84ER40150.

#### DISCLAIMER

This report was prepared as an account of work sponsored by the United States government. Neither the United States nor the United States Department of Energy, nor any of their employees, makes any warranty, express or implied, or assumes any legal liability or responsibility for the accuracy, completeness, or usefulness of any information, apparatus, product, or process disclosed, or represents that its use would not infringe privately owned rights. Reference herein to any specific commercial product, process, or service by trade name, mark, manufacturer, or otherwise, does not necessarily constitute or imply its endorsement, recommendation, or favoring by the United States government or any agency thereof. The views and opinions of authors expressed herein do not necessarily state or reflect those of the United States government or any agency thereof.

## POLARIZATION PHENOMENA IN ELECTROMAGNETIC INTERACTIONS AT INTERMEDIATE ENERGIES.

V. Burkert

Continuous Electron Beam Accelerator Facility, 12000 Jefferson Avenue, Newport News, Virginia 23606, USA.

**Resume.** Des résultats récents de mesures de polarisation en interaction électromagnétique aux énergies intermédiaires sont discutés. Les perspectives concernant les expériences de polarisation auprès des nouveaux accélérateurs d'électrons à courant continu, ainsi qu'auprès de machines plus anciennes améliorées, sont brièvement décrites. En conclusion, on montre que les expériences de polarisation vont jouer un rôle très important dans l'étude de la structure du nucléon et des noyaux légers.

**Abstract.** Recent results of polarization measurements in electromagnetic interactions at intermediate energies are discussed. Prospects of polarization experiments at the new CW electron accelerators, as well as on upgraded older machines are outlined. It is concluded that polarization experiments will play a very important role in the study of the structure of the nucleon and of light nuclei.

### I. INTRODUCTION.

In this talk I discuss some of the recent results in intermediate energy electromagnetic physics with polarized particles from an experimentalist point of view. Polarized hydrogen and deuterium targets as well as recoil polarimeters have been developed over the past several decades. These have become reliable experimental tools, and are used in various physics areas. Much of the recent experimental effort in electromagnetic physics has focussed on the nucleon and deuteron. With the development of  $^3\text{He}$  as a polarized quasi-neutron target one may expect extensive experimental studies of the 3-nucleon system to be carried out in the near term future. The physics possibilities using  $^3\text{He}$  as a target have been discussed in several presentations at this conference. My focus here is on the physics with hydrogen and deuterium targets, and I want to discuss the major experimental trends which have emerged over the past few years, mainly in support of the physics programs for the new CW electron machines that are presently under construction.

Of course, in electron scattering experiments "polarization" is always present, as a transverse polarization of the electric field vector of the virtual photon. To limit the scope of this talk, I will assume that the polarization of one of the external particles is measured.

### II. STRUCTURE OF THE NUCLEON.

The interest in the structure of the nucleon and its resonances, and their role in nuclear properties has dramatically increased in recent years and is one of the major motivations in support of the planned experimental program at the new electron machines. The structure of the nucleon may be probed in elastic electron nucleon scattering and in inelastic reactions induced by electrons or photons. These studies are of fundamental importance as they measure the charge and current distribution as well as the transition currents of the fundamental building blocks of matter. Knowledge of these quantities allows stringent tests of microscopic models applicable at low and intermediate energies, like QCD-based quark models, chiral bag models, Skyrme models, etc.. With increasing momentum transfer  $Q^2$  the transition from the non-perturbative regime to the perturbative regime can be studied, where simple quark counting rules may apply<sup>1</sup>.

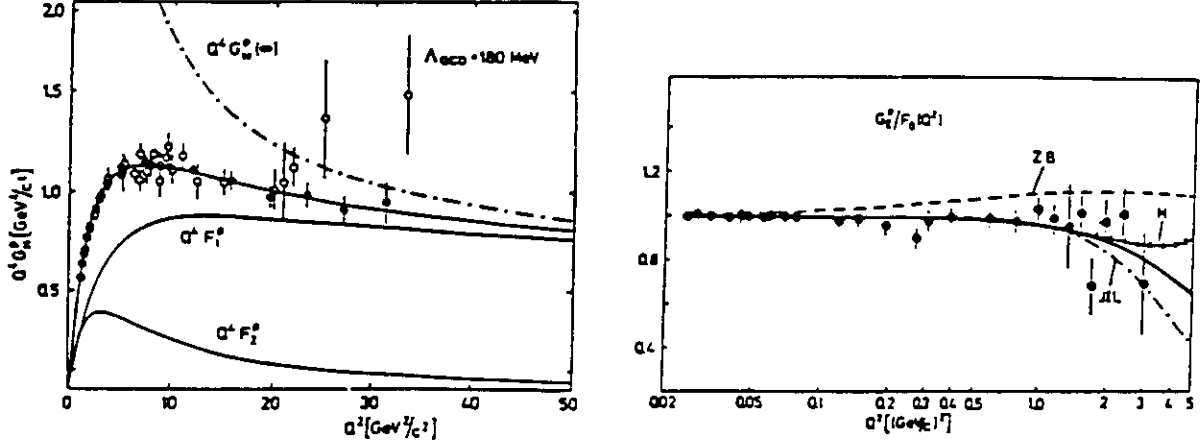


Figure II.1 Result of the QCD analysis of the proton elastic formfactors<sup>2</sup> using  $\Lambda = 180 \text{ MeV}$ . The solid line represents the fit to the data.

## II.1 Electromagnetic Formfactors.

In elastic electron nucleon scattering the hadronic current is specified by the electric and magnetic formfactors  $G_E(Q^2)$  and  $G_M(Q^2)$ . These are related to the Dirac and Pauli formfactors  $F_1$  and  $F_2$  as:

$$G_E = F_1 - \tau F_2, \quad G_M = F_1 + F_2$$

where  $\tau = \frac{Q^2}{4M^2}$ . The usual techniques for measuring the elastic formfactors is the Rosenbluth separation, where one makes use of the different angular dependence of the electric and the magnetic term in the unpolarized elastic cross section to separate  $|G_E|$  and  $|G_M|$ .

$$\frac{d\sigma}{d\Omega} = \left(\frac{d\sigma}{d\Omega}\right)_M \frac{E'}{E} [(G_E^2 + \tau G_M^2) + 2\tau(1 + \tau)G_M^2 t g^2 \frac{\theta}{2}]$$

This techniques ceases to be useful, when either  $G_E^2 \ll G_M^2$ , or at high values of  $Q^2$ , where the magnetic contributions dominate both the angular dependent and the angular independent terms. Experimental information on the neutron electric formfactor  $G_{En}$  is rather poor for all non-zero  $Q^2$ . In the absence of a free neutron target, we have to rely on scattering from the few-nucleon systems. Unlike for the proton, the Rosenbluth separation of  $G_{En}$  from  $G_{Mn}$  is difficult even at low  $Q^2$  because of the small size of  $G_{En}$  compared to  $G_{Mn}$ . At low  $Q^2$ ,  $G_{En}$  would be non-zero only if the charge distribution within the neutron were not uniform. The slope of  $G_{En}$  versus  $Q^2$ , at low  $Q^2$  has been accurately measured, and it is positive, indicating that the neutron appears to have a slightly positive core surrounded by a region of negative charge. For  $Q^2 < 1 \text{ GeV}^2$   $G_{En}$  has been extracted from elastic electron-deuteron scattering data<sup>2,3</sup>. Using this procedure, however, it is necessary to assume a model for the deuteron structure. The most recent analysis allows for a 15% systematic uncertainty in  $G_{En}$  for  $Q^2 < 0.8 \text{ GeV}^2$ . For larger values of  $Q^2$ , uncertainties in the deuteron wavefunction render the methods unreliable.

The electric formfactor of the proton has been measured at SLAC<sup>4</sup> using Rosenbluth separation for  $Q^2$  up to about  $4 \text{ GeV}^2$ , with error bars of 20% at the highest momentum transfer. The proton magnetic formfactor, on the other hand, has been measured for  $Q^2$  up to  $31 \text{ GeV}^2$ . An analysis of the electromagnetic formfactors by Gari and Stefanis<sup>5</sup> allowed extraction of the QCD scale parameter  $\Lambda_{QCD}$ . In lowest order  $\Lambda_{QCD}$  can be defined in relation to the strong coupling constant  $\alpha_s$ :

$$\alpha_s(Q^2) = \frac{12\pi}{(33 - 2n_f) \ln(Q^2/\Lambda_{QCD}^2)}$$

where  $n_f$  is the number of quarks with mass lower than  $Q^2$ . Assuming a conventional meson picture at small  $Q^2$ , and asymptotic QCD predictions at high  $Q^2$

$$F_1 = \frac{C_1}{Q^4} \quad , \quad F_2 = \frac{C_2}{Q^6} \quad ,$$

a fit to the electromagnetic formfactors (Figure II.1) yielded values for  $\Lambda_{QCD}$  between 100 - 250 MeV/c. The uncertainties are mainly due to the limited knowledge of  $G_{Ep}$  at  $Q^2 \geq 2\text{GeV}^2$ . A more precise determination of this parameter would be very interesting since  $\Lambda_{QCD}$  is not well determined from other measurements.

## II.2 Polarisation Techniques to Measure $G_{En}$ and $G_{Ep}$

Two methods appear very promising in that they allow measurement of  $G_{En}$  in a model independent fashion. Both methods employ quasi elastic scattering of polarised electrons off deuterium. In the first case polarised electrons are scattered off polarised deuterium<sup>6</sup>. In the second case an unpolarised deuterium target is used and the polarisation of the recoil neutron is measured in a second scattering experiment<sup>7</sup>. Both methods are equivalent, and allow measurement of the polarisation asymmetry

$$A_{en} = \frac{2\tau\cos\theta v'_T + 2\sqrt{2\tau(1+\tau)} \cdot (G_{En}/G_{Mn})\sin\theta\cos\phi v'_{TL}}{v_L(1+\tau)(G_{En}/G_{Mn})^2 + 2\tau v_T}$$

where  $v_L, v_T, v'_T, v'_{TL}$  are known kinematic quantities. By varying  $\theta$ , the angle between the nuclear spin and the direction of momentum transfer, it is possible to pick out the longitudinal and transverse pieces of the quasi elastic spin dependent cross section. In particular, if  $\theta = 90^\circ$ , the asymmetry is proportional to  $G_{En}/G_{Mn}$ . Knowing  $G_{Mn}$  the electric formfactor can be determined.

The first method uses a polarised deuterium (or  $^3\text{He}$ ) target, either as a ultra thin gas target<sup>8,9</sup> in an electron storage ring, or a solid state target ( $\text{ND}_3$ )<sup>10,11,12</sup>, or a dense  $^3\text{He}$ <sup>13,14</sup> gas target, in an external electron beam. In case the polarisation asymmetry is measured using vector polarised deuterium, it will be necessary to measure the recoil neutron in coincidence with the scattered electron to veto against the much larger asymmetry effects from the polarised proton in the deuteron. Model calculations<sup>15,16</sup> show (Figure II.2) that the polarisation asymmetry is linearly dependent on  $G_{En}/G_{Mn}$  as long as the recoil neutron is

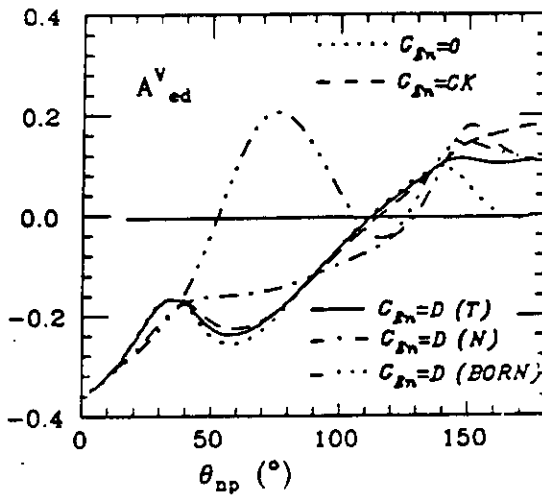


Figure II.2 Double polarization asymmetry  $A_{ed}$  for various assumptions on  $G_{en}$ , and different interaction models<sup>15</sup>.

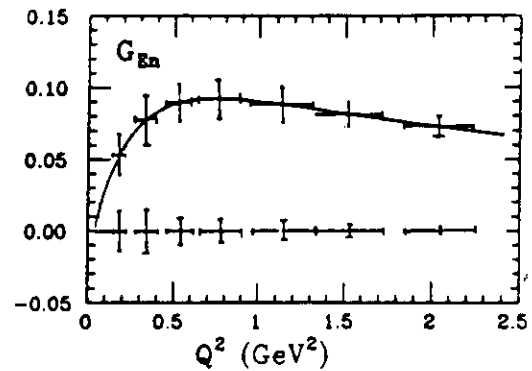


Figure II.3 Projected data for a measurement of  $G_{en}$  at CEBAF using recoil polarization techniques<sup>70</sup>.

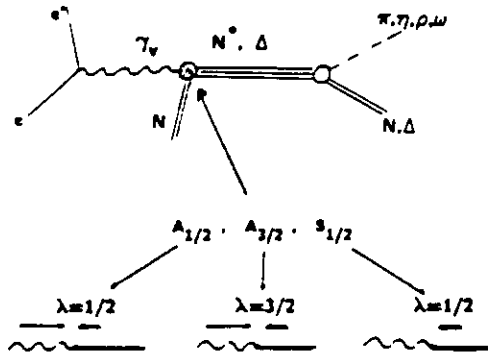


Figure II.4 Electroproduction of hadronic final states via  $s$ -channel resonance decays. The  $\gamma NN^*$  vertex is described by the photocoupling helicity amplitudes  $A_{1/2}$ ,  $A_{3/2}$ ,  $S_{1/2}$ .

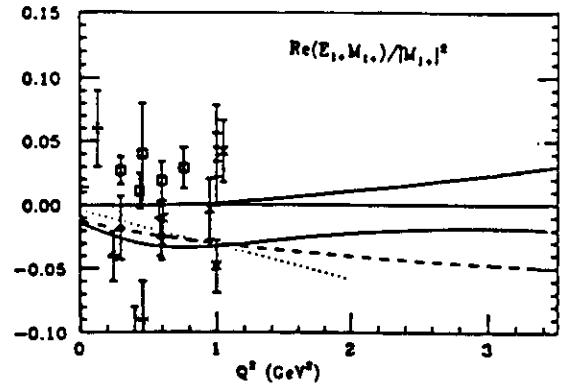


Figure II.5 Comparison of experimental data on the interference term  $\text{Re}(E_{1+} M_{1+}) / |M_{1+}|^2$  for the  $\Delta(1232)$  with various model calculations.

emitted at small angles with respect to the direction of the virtual photon. In this region the influence of the deuteron wave function on the extracted value of  $G_{E_n}/G_{M_n}$  is almost absent. A quantitative check can be accomplished by measuring the proton asymmetry at the same time, and by comparing it to the asymmetry obtained with a polarised hydrogen target (e.g.  $\text{NH}_3$ ). For  $^3\text{He}$  nuclear corrections are not negligible<sup>17</sup> and will have to be carefully studied when extracting  $G_{E_n}$ .

Employing state of the art polarised target technology it appears feasible to measure  $G_{E_n}$  for  $Q^2$  up to  $0.5 \text{ GeV}^2$  with a  $1 \text{ GeV}$  electron beam, and up to  $2$  or  $3 \text{ GeV}^2$  using a  $4 \text{ GeV}$  beam. Projected error bars for a measurement at CEBAF which employs the recoil polarisation techniques are shown in Figure II.3.

The polarisation techniques discussed above can also be used to measure the electric formfactor  $G_{E_p}$  of the proton. Most promising in this respect appears to be the recoil polarisation techniques using an unpolarised hydrogen target<sup>18</sup>, and the measurement using a polarized  $\text{NH}_3$  target<sup>19</sup>. With a  $4 \text{ GeV}$  beam values of  $Q^2$  up to  $5 \text{ GeV}^2$  can be reached with either techniques. Recent achievements in polarized target technology<sup>20</sup> may allow one to push this limit to even higher values.

### II.3 Nucleon Resonance Transition Formfactors

A large number of resonances, attributed to the excitation of the nucleon have been observed in hadron scattering, the  $\Delta(1232)$  being the most prominent one. Electroexcitation of resonances on the free nucleon yields information on the  $\gamma_v NN^*$  vertex as a function of  $Q^2$  (Figure II.4). The transition into a specific excited state is described by three amplitudes  $A_{1/2}(Q^2)$ ,  $A_{3/2}(Q^2)$ ,  $S_{1/2}(Q^2)$ , where A and S refer to transverse and scalar coupling, respectively, and the subscripts refer to the total helicity of the  $\gamma_v N$  system (frequently, the electromagnetic multipoles  $E_{l\pm}$ ,  $M_{l\pm}$ ,  $S_{l\pm}$  are used instead). Inclusive measurement of  $\gamma N \rightarrow X$ , or  $eN \rightarrow eX$  reveal a few broad bumps, clearly indicating the excitation of resonances in the mass region below  $2 \text{ GeV}$ . Their broad widths and close spacing makes it impossible to separate them in inclusive production reactions. By explicit measurement of the decay products such as  $\pi N$ ,  $\eta N$ ,  $\rho N$ ,  $\pi \Delta$ , and others, it is possible to identify them according to their spin and isospin assignments.

The physics issues one hopes to study are manifold, and address fundamental questions about the interaction of quarks and gluons in confined systems. Specifically, one would like to study how the transition between the 3-quark ground state and excited states is mediated. Most models assume that the excitation is due to a single quark transition. However, recent studies<sup>21</sup> indicate that double quark transitions may be present at a non-negligible level. Measurement of the  $Q^2$  evolution

of the transition formfactors provides information about the wave function of the excited state. The helicity asymmetry

$$A_{1/2,3/2} = \frac{A_{1/2}^2 - A_{3/2}^2}{A_{1/2}^2 + A_{3/2}^2}$$

for the transition into some excited states, like the  $D_{13}(1520)$ , or  $F_{15}(1688)$ , was found to be sensitive to the potential that confines the valence quarks inside the nucleon<sup>21</sup>. At high momentum transfer one may observe the transition from the non-perturbative to the perturbative regime, where power law rules for the helicity amplitudes are predicted to apply<sup>22</sup> such that:

$$A_{1/2} = C_1/Q^3, \quad A_{3/2} = C_2/Q^5, \quad Q^2 \rightarrow \infty$$

if logarithmic terms are neglected. Whether this regime can be reached at the available energies (e.g. 4 GeV at CEBAF) is an open question. None the less, it will be interesting to push studies of the helicity structure of nucleon resonance excitations to the highest possible  $Q^2$ .

The QCD motivated extension of the non-relativistic quark-model<sup>23</sup> predicts many states, in particular at higher masses, which have not been observed in  $\pi N$  reactions. Theoretical calculations<sup>24</sup> indicate that the "missing" states tend to decouple from the  $\pi N$  channel, which would explain why they have not been seen in elastic  $\pi N$  scattering. Our picture of baryon structure could drastically change if these states did not exist. Several of these states are predicted to couple strongly to photons (real or virtual) and may thus be searched for in photo- or electroproduction experiments. A complete program to study nucleon resonance transitions, e.g. in  $\gamma_e N \rightarrow \pi N$ , involves measurement of 6 (4 in photoproduction) complex, parity conserving amplitudes.

$$H_i := \langle \lambda_\pi; \lambda_N | T | \lambda_{\gamma_e}; \lambda_p \rangle = \langle 0; \pm \frac{1}{2} | T | \pm 1, 0; \pm \frac{1}{2} \rangle$$

which makes it necessary to measure at least 11 independent observables, not counting additional measurements to resolve quadratic ambiguities. Experiments involving unpolarised particles only, allow measurement of only 4 response functions  $\sigma_T, \sigma_L, \sigma_{TT}, \sigma_{LT}$ :

$$\frac{d\sigma}{d\Omega} = \sigma_T + \epsilon\sigma_L + \epsilon\sigma_{TT}\cos 2\phi + \sqrt{2\epsilon(1+\epsilon)}\sigma_{LT}\cos\phi, \quad \sigma_i = \sigma_i(H_1, \dots, H_6)$$

Measurement of polarization observables yield information on many response functions (table)

Response Functions in Electron Scattering	
Experiment	# Response Functions
unpol. cross section	4
polarised e beam	1
polarised target	8
pol. beam/pol. target	5
recoil polarisation	8
pol. beam/recoil pol.	5

I want to illustrate the significance of polarization measurements for this program with two examples, the  $\gamma_e p \Delta^+(1232)$  and the  $\gamma_e p P_{11}^+(1440)$  transitions.

### II.3.1 The Transition $\gamma_e p \rightarrow \Delta^+(1232) \rightarrow N\pi$ .

In SU(6) symmetric quark models this transition is explained by a simple quark spin-flip in the  $L_{3Q} = 0$  ground state, corresponding to a magnetic dipole transition  $M_{1+}$ . The electric and scalar quadrupole transitions are predicted to be  $E_{1+} = S_{1+} = 0$ . In more elaborate QCD based models which include color magnetic interaction arising from the one-gluon exchange at small distances, the  $\Delta(1232)$  acquires an  $L_{3Q} = 2$  component, leading to small electric and scalar quadrupole contributions (e.g.  $|E_{1+}/M_{1+}| \simeq 0.01$  at  $Q^2 = 0$ ). The ratio  $|E_{1+}/M_{1+}|$  is predicted to be weakly dependent on  $Q^2$ . At very high  $Q^2$  QCD predicts<sup>25</sup>  $E_{1+}/M_{1+} \rightarrow 1$ , and  $S_{1+}/M_{1+} \rightarrow 0$ . Precise measurements of these contributions from  $Q^2 = 0$  to very large  $Q^2$  are obviously important for the development of realistic models of the nucleon. Present experimental information about  $E_{1+}$  is shown in Figure II.5, together with model predictions. The quality of the data is clearly not sufficient to discriminate against any of the models. Experiments at MIT-Bates<sup>26</sup> and CEBAF<sup>27</sup> are in preparation to measure the electric and scalar quadrupole transition over a large  $Q^2$  range, using polarised electron beams and/or recoil polarimeters. In these experiments one obtains information about the terms

$$M_{1+}, \text{Re}(E_{1+}M_{1+}^*), \text{Re}(S_{1+}M_{1+}^*), \text{Im}(E_{1+}M_{1+}^*), \text{Im}(S_{1+}M_{1+}^*).$$

The imaginary parts of the bilinear terms can only be accessed using polarisation degrees of freedom. They are particularly sensitive to phase relations between the multipoles. If the multipoles were strictly in phase, these terms would vanish identically.

### II.3.2 The Transition $\gamma_e p \rightarrow P_{11}^+(1440) \rightarrow N\pi$ .

The Roper resonance  $P_{11}$  has a modestly strong photocoupling at  $Q^2 = 0$ , but in electron scattering there is little evidence for its excitation both, in the inclusive cross section and in exclusive single pion production at  $Q^2 < 1\text{GeV}^2$ . In an analysis<sup>28</sup> of single pion production data at  $Q^2 = 1\text{GeV}^2$ , a small positive value was found for the  $A_{1/2}(P_{11})$  amplitude. At  $Q^2 = 0$  this value is larger and negative. One may speculate that the apparent quenching of the Roper at  $Q^2 > 0$  might be accidental and related to a zero crossing of the transverse amplitude. The  $P_{11}$  may then be expected to "reappear" at higher  $Q^2$ . In fact, non-relativistic<sup>29</sup> as well as relativised<sup>21</sup> quark models predict the  $A_{1/2}(P_{11})$  amplitude to grow relative to the  $\Delta(1232)$ . In non-relativistic models  $A_{1/2}(P_{11})/A_{1/2}(\Delta) \sim Q^2$ , so that the  $P_{11}$  would dominate at high  $Q^2$ .

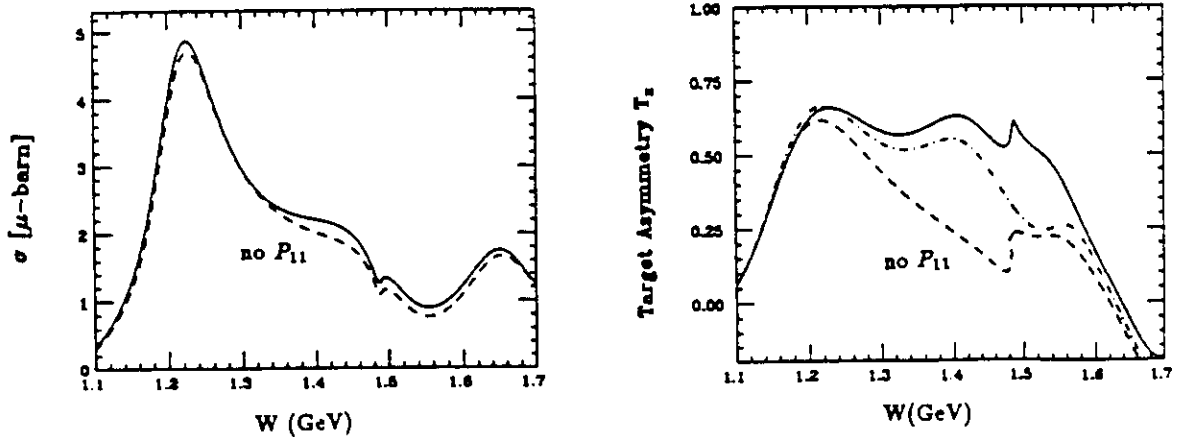


Figure II.6 Predicted cross section for  $\gamma_e p \rightarrow \pi\pi^0$  at  $Q^2 = 1\text{GeV}^2$ ,  $\epsilon = 0.8$ ,  $\theta_\pi^* = 0^\circ$ , using the amplitudes of G. Kroesen<sup>28</sup>. The sensitivity to the (small) amplitudes of the Roper resonance is shown (left). Predicted target asymmetry  $T_n$  for the same kinematics (right). The sensitivity to the Roper and the  $S_{11}(1535)$  is shown. The dashed-dotted line is obtained when the nearby  $S_{11}$  resonance amplitudes are switched off. Note that the dominant  $S_{11}$  amplitude is known to better than 20%.

It has been pointed out that the dominance of the  $P_{11}$  at high  $Q^2$  will be a crucial test of the quark model classification as a  $N=2$  radially excited state<sup>29</sup>. Measurements with polarized proton targets<sup>19</sup>, or proton recoil polarization measurements<sup>30</sup> can provide a strong signature for the excitation of this resonance in electron scattering experiments. Figure II.6 shows the sensitivity of the unpolarized cross section and the polarized target asymmetry  $T_e$  in  $\gamma, p \rightarrow p\pi^0$  to the  $P_{11}$  amplitudes. Clearly, measurement of polarisation observables will have an important impact on the determination of the photocoupling amplitudes of the Roper.

## II.4 Meson Photoproduction from Nucleons

### II.4.1 Photoproduction of $\pi$ Mesons.

Single pion photoproduction experiments have a long history, and a large body of data has been generated over more than two decades of experiments at various laboratories. The goal has been to extract the 4 complex helicity amplitudes  $H_1, \dots, H_4$  that completely specify the single pion production process. Data are needed in different isospin channels, like  $\gamma p \rightarrow p\pi^0$ ,  $\gamma p \rightarrow n\pi^+$ , and  $\gamma n \rightarrow p\pi^-$ . Such a complete set of data would then allow one to determine the photocoupling amplitudes of the  $N^*$  and  $\Delta$  resonances in a model independent fashion. At least 9 independent measurements are needed at each kinematic point  $(E_\gamma, \theta_\pi^*)$ , including 5 double polarisation measurements<sup>31</sup>. Much cross section data and single polarisation data have been accumulated, and recent measurements have focussed on obtaining the missing information from the double polarisation experiments. Figure II.7 and II.8 show recent results<sup>32,33</sup> from the Yerevan 4.5 GeV electron synchrotron, in the  $2_{n,d}$  and  $3_{r,d}$  nucleon resonance region. The sensitivity to the ingredients of various phenomenological analysis is shown as well. The same analysis that correctly predicted the  $p\pi^0$  results, fails in the  $n\pi^+$  channel, which demonstrates the importance of measurements in different isospin channels. Unfortunately, the impact of this data on an extraction of the resonant amplitudes in a phenomenological fit would likely be small, because of the large error bars.

### II.4.2 Photoproduction of $\eta$ Mesons.

At the Bonn stretcher ring ELSA preparations are under way to measure the target asymmetry in the reaction  $p(\gamma, p)\eta$  in the region of the  $S_{11}(1535)$  nucleon resonance<sup>34</sup>. Only two of the known nucleon resonances, the  $S_{11}(1535)$ , and the  $P_{11}(1710)$ , have a significant branching ratio into the  $N\eta$  channel. The  $P_{11}(1710)$  has been proposed as a possible candidate for a hybrid state<sup>35</sup> (three valence quarks, one valence gluon). Precise measurements of the photocoupling amplitudes for proton and neutron targets are needed to clarify the assignment of this state as a conventional  $Q^3$  or an exotic  $Q^3G$  state. If the  $P_{11}(1710)$  is a hybrid state then  $A_{1/2}^p(P_{11}) = 0$ , and  $A_{1/2}^n(P_{11}) \neq 0$ . An experimental program, including polarization measurements, for a complete measurement of this channel should prove extremely interesting, and would be far less complex than the corresponding program for the  $N\pi$  channel.

### II.4.3 Photoproduction of Strange Particles.

At CEBAF a program to study the reaction  $\gamma p \rightarrow K^+\Lambda \rightarrow p\pi^-$  is in preparation. This reaction has been studied very poorly in the past, with the result that the production mechanism is not understood. If one takes a diagrammatic approach, one can hope to extract information about the  $K\Lambda N$  and  $K\Lambda N^*$  coupling constants. Coupling constants, extracted from existing photoproduction data disagree with the ones extracted from hadronic processes. Recent calculations<sup>36</sup> indicate that measurement of the  $\Lambda$  recoil polarization, as well as measurement of the beam asymmetry, are very sensitive to specific ingredients of the model, and assumptions about the coupling constants.

An efficient experimental program to study polarisation degrees of freedom in the  $K\Lambda$  channel requires use of large acceptance detectors with nearly  $4\pi$  solid angle coverage. At CEBAF such a detector is under construction for one of the three experimental endstations. With such an instrument, detailed polarization data can be obtained for this reaction. For example, the  $\Lambda$  polarization can be inferred from an analysis of its  $\pi^- p$  decay. Using a longitudinally polarized electron beam, circularly polarized bremsstrahlung photons can be generated, and the polarization transfer reaction  $\bar{\gamma}p \rightarrow K\bar{\Lambda}$  can be studied as well.

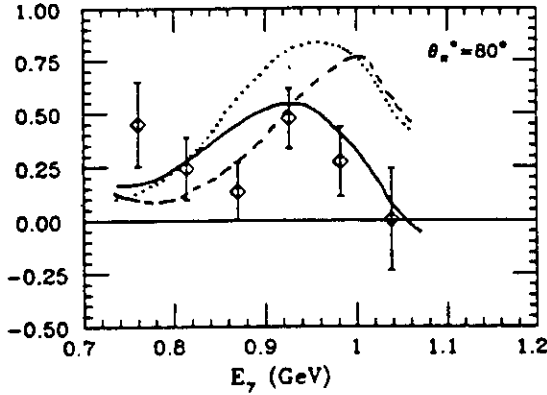


Figure II.7 Double polarization asymmetry  $O_x$  at  $\theta_n^* = 80^\circ$  for the process  $\gamma p \rightarrow \pi^+ n$  in the region of the  $2_{n_4}$  and  $3_{n_4}$  nucleon resonance. Data from Yerevan<sup>32</sup>. The curves are predictions of phenomenological analyses. Solid line: Metcalf and Walker<sup>71</sup>

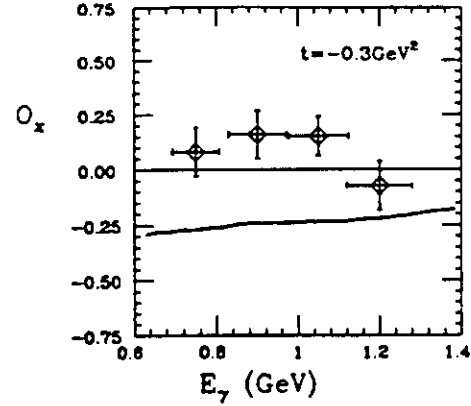


Figure II.8 Double polarization asymmetry  $O_x$  for  $\gamma p \rightarrow \pi^+ n$ . Data from Yerevan<sup>32</sup>. Same calculation as in Figure II.7.

#### II.4.4 Drell-Hearn Gerasimov Sum Rule.

The result of the polarised proton structure functions measurement has triggered new interest<sup>29,37</sup> in experimental tests of the sum rule of Drell-Hearn<sup>38</sup> and Gerasimov<sup>39</sup>:

$$\int_{\nu_{thr}}^{\infty} \frac{d\nu}{\nu} [\sigma_{1/2}(\nu, 0) - \sigma_{3/2}(\nu, 0)] = -\frac{2\pi^2\alpha}{M^2} k^2,$$

where  $\nu$  is the photon energy,  $\sigma_{1/2}$  and  $\sigma_{3/2}$  are the absorption cross sections for total helicity 1/2 and 3/2, and  $k$  is the anomalous magnetic moment of the target nucleon. The sum rule has been derived on rather general grounds but has never been tested experimentally, although an analysis of single pion production experiments allows to place some limits on by how much it may be violated<sup>40</sup>. Using a circularly polarised tagged photon beam, generated by longitudinally polarised electrons, and polarised  $NH_3$  as target material, the total absorption cross section difference  $\sigma_{1/2} - \sigma_{3/2}$  can directly be measured as a function of the photon energy. The integral is weighted by  $1/\nu$ , therefore the lower energy regime, in particular the resonance region give the largest contributions. Existing or planned medium energy accelerators are the appropriate instruments for testing this sum rule.

### III. STRUCTURE OF THE DEUTERON.

#### III.1 Elastic Electron-Deuteron Scattering

In elastic eD scattering, the hadronic current is specified by 3 isoscalar electromagnetic formfactors,  $G_C$ ,  $G_Q$ ,  $G_M$ , which are related to the charge, electric quadrupole moment, and magnetic dipole moment, respectively. The charge formfactor, in particular, is very sensitive to the short range part of the N-N potential, and to the size of isoscalar meson exchange currents. Rosenbluth separation of the unpolarised elastic eD scattering cross section allow separation of

$$G_M^2, G_C^2 + \frac{8}{9}\tau^2 G_Q^2; \quad \tau = Q^2/4M_D^2.$$

Information about  $G_C$  and  $G_Q$  separately can only be obtained in measurements of polarisation observables.

In the absence of a polarized electron beam, one can either measure the tensor polarization components of the recoil deuteron in  $D(e, e'D)$ , or alternatively measure the analyzing power in  $\bar{D}(e, e'D)$ .

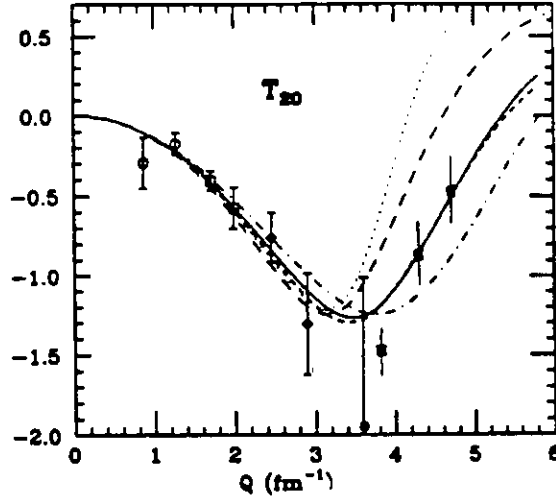


Figure III.1 Experimental results on the analyzing power  $T_{20}$  for  $eD \rightarrow eD$ . The data are compared with various model calculations. For a detailed discussion see M. Garcon<sup>72</sup>.

The first method was used in two measurements at MIT-Bates<sup>41,42</sup>. The second method was employed in experiments at the Novosibirsk VEPP-2 and VEPP-3 storage rings<sup>43,44</sup> with a polarized  $D_2$  gas target. A Bonn group, working at the 2.5 GeV synchrotron used a dynamically polarized  $ND_3$  target<sup>45</sup>. For a tensor polarized target the elastic scattering cross section is given by:

$$\frac{d\sigma}{d\Omega} = \left(\frac{d\sigma}{d\Omega}\right)_0 [1 + T_{20}t_{20} + 2T_{21}Re(t_{21}) + 2T_{22}Re(t_{22})]$$

$T_{20}$  appears to be most sensitive to  $G_C$ . If the magnetic component can be neglected (at forward angles, and  $\tau G_M^2 \ll G_C^2$ ,  $\tau^2 G_Q^2$ )

$$T_{20} \simeq -\sqrt{2} \frac{\frac{2}{3}\tau G_Q(\frac{2}{3}\tau G_Q + 2G_C)}{G_C^2 + \frac{8}{9}\tau^2 G_Q^2}$$

The interference term  $G_C G_Q$  makes  $T_{20}$  a particularly suitable quantity to measure. Figure III.1 shows the present experimental situation. Only the most recent results from MIT-Bates have sufficient sensitivity to allow discrimination between some of the models. Clearly, the asymptotic scaling model<sup>46</sup> which predicted  $T_{20}$  to asymptotically approach the value  $-\sqrt{2}$  is ruled out in the  $Q^2$  range where data are available.

As we have heard during this conference<sup>44</sup> new measurements are being planned at Novosibirsk with 100 times higher target densities. Also, polarized solid state target technology has advanced to a point where improvements of similar magnitude appear feasible<sup>20</sup>. These advances may allow to push the measurements to higher momentum transfer, as well as to improve the statistical significance at lower  $Q^2$ .

## III.2 Disintegration of the Deuteron

### III.2.1 Photodisintegration

To a large degree recent polarization measurements have been prompted by the observation of an unexpectedly large proton recoil polarization seen in a Tokyo experiment<sup>47</sup> near 550 MeV photon energy. The result was interpreted as an indication for the excitation of intermediate dibaryon states. In the energy region of the  $\Delta(1232)$  new measurement of the proton recoil polarization have become available from Kharkov<sup>44</sup> (Figure III.2), which allow to test various model calculations. In general,

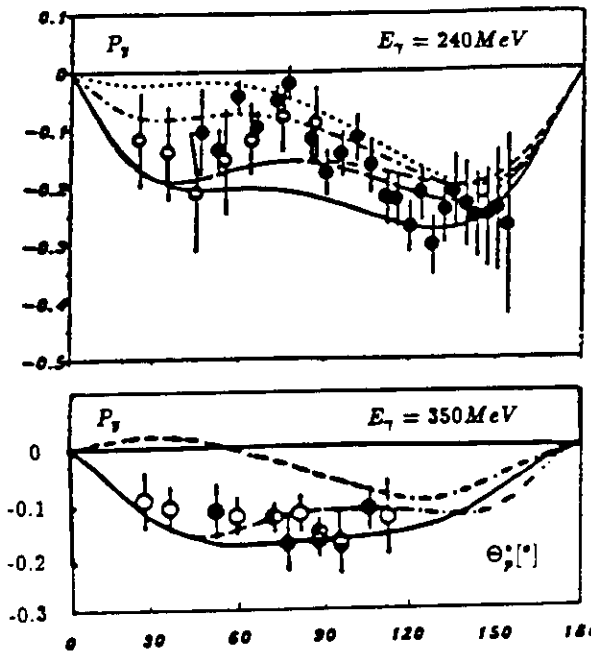


Figure III.2 Recent results on proton recoil polarization measurements in deuteron photo disintegration<sup>48</sup>, and polarized neutron capture. Top: Non-relativistic calculations using various NN potentials: Bonn (dotted), Argonne V14 (dashed-dotted), Argonne V28 (short dashes), RSC (long dashes), RSC/nSO (solid). Bottom: Coupled channel calculations by Tanabe & Ohta<sup>50</sup> (dotted), and Leidemann & Arenhovel<sup>49</sup> (IA: dashed, IA+IC: dashed-dotted, IA+IC+MEC: solid).

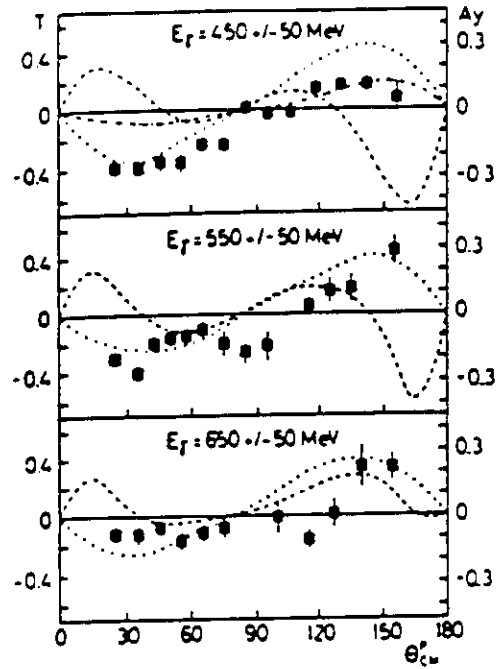


Figure III.3 Bonn data<sup>51</sup> on the analyzing power  $A_y$  in deuteron photodisintegration using a polarized  $ND_3$  target. Non-relativistic calculations by Leidemann & Arenhovel<sup>49</sup> (dashed-dotted), and relativistic calculations by Laget<sup>52</sup> (dashed), and Kang<sup>51</sup>. Note that the calculations agree on the position of the zero crossing.

non-relativistic calculations describe the data well, when IC and MEC are included, in a coupled channel approach<sup>46</sup>, or in unitary theory<sup>45</sup>, and there is no apparent need for including dibaryon states into the calculation.

Figure III.3 shows results of a target asymmetry measurement carried out at the Bonn 2.5 GeV synchrotron<sup>51</sup> using a polarized  $ND_3$  target. The data exhibit an energy dependence, which can presently not be explained in calculations using conventional models. A partial wave fit indicates that the angular distribution at 550 MeV requires a  $J_{\text{max}} = 2$  angular momentum contribution, which could indicate the excitation of an intermediate  $J=2$  state. However, in the analysis of the Tokyo data  $J_{\text{max}} = 4$  yielded the best fit. It would clearly be desirable to collect good statistics data in smaller energy bins that would allow one to study the energy dependence in more detail. Also, analyses that make use of all existing data including angular distributions of the unpolarized cross section, could provide better constraints on exotic contributions to the process.

Polarized photon asymmetries have recently been measured at the Yerevan synchrotron<sup>53</sup>. An energy spectra is shown in Figure III.4. The  $90^\circ$  low energy data ( $\leq 0.5\text{GeV}$ ) can be described by conventional model calculations. An interesting feature is the apparent failure of the coupled channel calculation<sup>49</sup> compared to the impulse approximation result in the same model. The data extend to 1GeV photon energy, and there is a clear need for the development of theoretical models in the higher energy regime. If one displays the beam asymmetry difference

$$\Delta\Sigma = \Sigma(180^\circ - \theta_p^{\text{cm}}) - \Sigma(\theta_p^{\text{cm}})$$

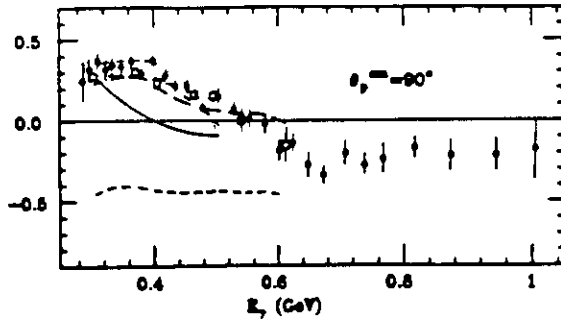


Figure III.4 Beam asymmetry  $\Sigma$  for deuteron photodisintegration. Data from Adamian et al.<sup>56</sup>. Calculation by Leidmann & Arenhove<sup>50</sup> (IC: dotted, full CC: solid), and Laget<sup>53</sup> (dashed-dotted). The lines that extend to 0.6 GeV are the result of a phenomenological analysis that includes various dibaryon states. (dashed line: nonresonant contributions only).

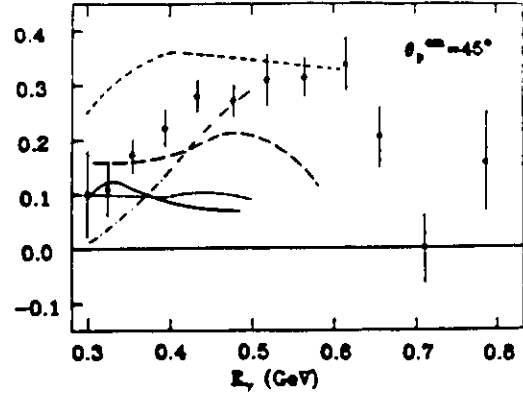


Figure III.5 Beam asymmetry difference  $\Sigma(45^\circ) - \Sigma(135^\circ)$ . Same calculations as in Figure III.4.

one is able to test isospin properties of the  $\gamma D \rightarrow pn$  amplitudes. The generalised Pauli principle requires  $\Delta\Sigma = 0$  for pure isospin states. Non-zero values indicate interferences between isoscalar and isovector amplitudes. The data are shown in Figure III.5. Some theoretical calculations that reproduce the beam asymmetry data<sup>40</sup> at  $90^\circ$  reasonably well, clearly fail to pass this isospin test. The calculation by Laget<sup>53</sup> that includes the  $P_{11}(1440)$  baryon resonance does comparatively better, which indicates that the excitation of higher mass resonances with isospin  $\frac{1}{2}$  ( $P_{11}(1440)$ ,  $S_{11}(1533)$ ) may play an important role in this process.

### II.2.2 "High Energy" Photodisintegration

Recently, there has been much speculation about the result of an experiment carried out at SLAC<sup>54</sup>, where the photodisintegration cross section was measured for energies up to 1.55 GeV. A striking feature is that around 1 GeV the data appear to follow the power law behaviour of

$$\frac{d\sigma}{dt} \propto \frac{1}{s^{11}},$$

( $\sqrt{s}$  is the cms energy) that was predicted by dimensional quark counting rules (Figure III.6).

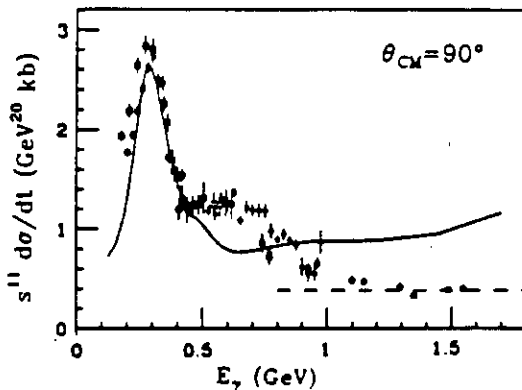


Figure III.6 Deuteron photodisintegration cross section multiplied by  $s^{11}$ . The data indicate dimensional scaling for energies above 1 GeV. Model calculation by T.S. Lee<sup>55</sup>.

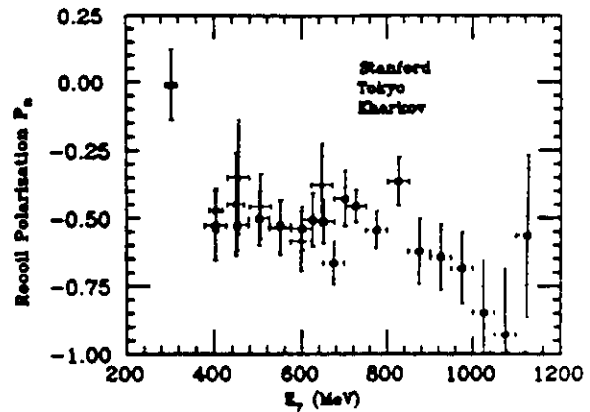


Figure III.7 Proton recoil polarisation in deuteron photodisintegration at  $\theta_{c.m.} = 120^\circ$ .

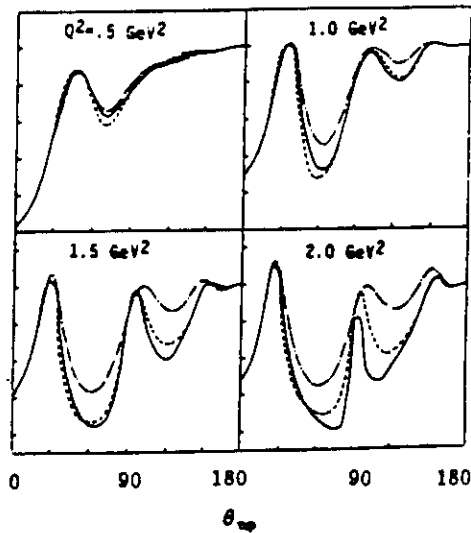


Figure III.8 Double polarization asymmetry for deuteron disintegration in quasi elastic  $eD$  scattering. Predictions by Rekalov<sup>16</sup> using RIA. The sensitivity to various assumptions about the NN potential is shown: Paris: solid, RSC: dashed, Buck-Gross: dash-dotted

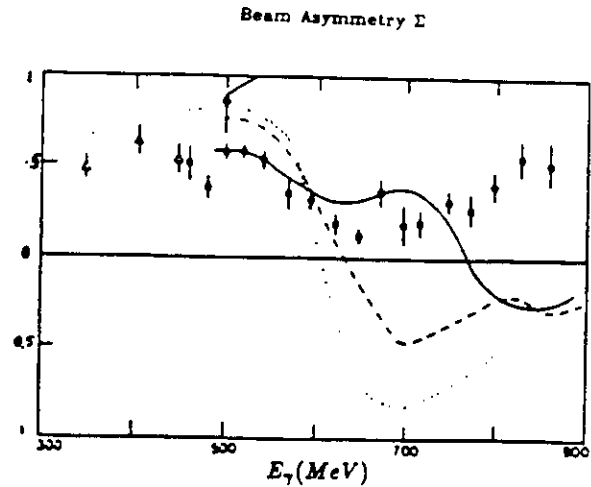


Figure III.9 Beam asymmetry in coherent  $\pi^0$  production from deuterium. Data from Adamian et al.<sup>61</sup>. The calculations include IA (dotted), and IA+RS (dashed). The solid line includes various dibaryon states, e.g.  $^3F_3(2260)$ ,  $^1G_4(2510)$ .

A calculation based on conventional theory<sup>56</sup> fails to reproduce this particular behaviour. We may ask the question, what we can learn about the process by looking at polarisation observable. At asymptotic energies QCD makes a simple prediction<sup>56</sup> about the nucleon recoil polarisation:  $P_n \rightarrow 0$ . Proton recoil polarisation data relevant for this discussion have in fact been measured at Kharkov<sup>57</sup>. Some of the data are shown in Figure III.7. The trend is obviously quite different from the asymptotic QCD predictions; the data show nearly maximum recoil polarisation at high energies,  $P_n \rightarrow -1$ . These results are obviously in serious disagreement with the simple counting rule interpretation of the cross section data.

### III.2.3 Electrodisintegration

Unpolarised measurements of the electrodisintegration reaction have revealed the importance of mesonic exchange reactions near the threshold for deuteron breakup<sup>58</sup>. Other measurements have revealed the importance of  $\Delta$  isobar contributions<sup>59</sup>. The study of polarisation observables is largely a matter of future experiment. At MIT-Bates and CEBAF experiments are under consideration to study this reaction using polarised electrons, proton recoil polarimeters, and vector polarised deuterium targets, in non-parallel kinematics.

$$D(\vec{e}, ep)n \quad (1), \quad D(\vec{e}, e\vec{p})n \quad (2), \quad \vec{D}(\vec{e}, ep)n \quad (3)$$

The first process yields new information only when the measurement is carried out in out-of-plane kinematics, where the proton is measured out of the electron scattering plane. A number of theoretical studies have been carried out<sup>15,16,60</sup> indicating that the reaction (1) is largely sensitive to final-state interactions, whereas (2) and (3) may reveal properties of the deuteron wavefunction, and of meson exchange contributions. Some of the results are displayed in Figure III.8, which shows the double polarization asymmetry for the reaction (3) in quasi-elastic kinematics. With increasing  $Q^2$  the asymmetry becomes very sensitive to assumptions about the NN potential and MEC's.

### III.3 Coherent $\pi^0$ Photoproduction from Deuterons

Another source of information about the two-nucleon system is coherent  $\pi^0$  production off deuterons  $\gamma D \rightarrow D\pi^0$ . The process is sensitive to the  $\pi NN$  dynamics in the two-nucleon system, and to possible excitations of dibaryon resonances. This reaction has recently been studied at Yerevan, using a linearly polarised coherent bremsstrahlung beam<sup>61</sup>. The results are shown in Figure III.9. Theoretical models that include impulse approximation (IA) and rescattering terms (RS) describe the beam asymmetry  $\Sigma$  qualitatively for energies up to about 600 MeV. At higher energies the theoretical description fails qualitatively, even when predicted dibaryon states are included in the calculation. Lack of knowledge of the deuteron wavefunction at short distances may, in part, be responsible for this discrepancy.

### IV. PHOTOPRODUCTION OFF LIGHT NUCLEAR TARGETS.

Data on polarisation observables become very sparse for nuclei other than the deuteron. Also, the interpretation of the data becomes more ambiguous as final state interactions become increasingly important. However, in some cases, one may be able to reduce effects from FSI by measuring polarisation asymmetries. A Kharkov group<sup>62</sup> has studied the beam asymmetry for various nuclei in  $(\gamma, \pi^\pm)$  and  $(\gamma, p)$  reactions, for energies in the region of the  $\Delta(1232)$ , where strong pion absorption usually prohibits the study of the initial photo-absorption mechanism, when pions are detected in the final state. When measuring the polarised beam asymmetry

$$\Sigma = \frac{\sigma_T(\pi^\pm) - \sigma_P(\pi^\pm)}{\sigma_T(\pi^\pm) + \sigma_P(\pi^\pm)}$$

FSI largely drop out in the ratio. The results for  $(\gamma, \pi^-)$  are shown in Figure IV.1.  $\Sigma$  is nearly independent of the target mass, which indicates that a quasi-free production mechanism dominates.

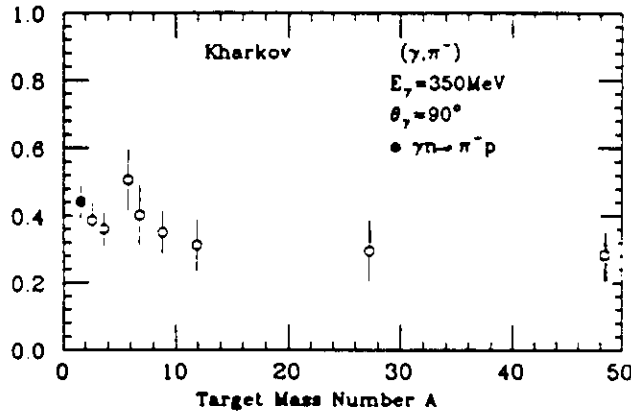


Figure IV.1 Beam asymmetry in the  $\Delta(1233)$  region, for inclusive  $\pi^-$  production from nuclei. Data from Zyalov et al.<sup>48</sup>.

### V. PARITY VIOLATION IN ELECTRON SCATTERING EXPERIMENTS.

In low and medium energy ( $Q^2 \ll M_Z^2$ ) neutral current interactions the parity violating contributions arise from the interference between the one-photon exchange and the neutral weak boson  $Z^0$  exchange graphs (Figure V.1). In electron scattering the interaction contains an isoscalar as well as an isovector piece in both, the vector ( $V_\mu$ ) and the axial vector ( $A_\mu$ ) coupling. The relevant piece of the Lagrangian can be written like

$$L_{pe} = \frac{G_F}{\sqrt{2}} \cdot [\bar{e}\gamma_\mu\gamma_5e(\bar{\alpha}V_\mu^3 + \tilde{\gamma}V_\mu^0) + \bar{e}\gamma_\mu e(\bar{\beta}A_\mu^3 + \tilde{\delta}A_\mu^0)]$$

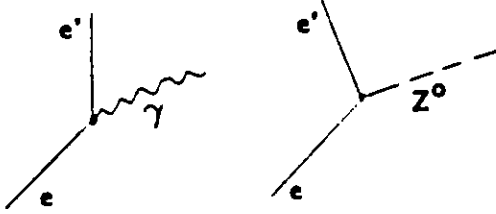


Figure V.1 Lowest order Feynman diagrams which contribute to parity non-conservation in electron scattering at low and intermediate energies.

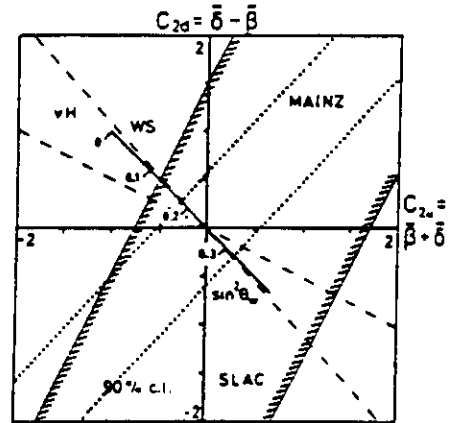


Figure V.2 Diagram for the quark coupling constants  $C_{2d}$  and  $C_{2u}$ . The areas allowed by the Mainz and SLAC experiments, and by neutrino-hadron scattering are indicated.

where  $\bar{\alpha}$ ,  $\bar{\beta}$ ,  $\bar{\gamma}$ ,  $\bar{\delta}$  denote the electro-weak coupling constants which have to be determined experimentally. By choosing appropriate kinematical conditions for electron scattering from nucleons and nuclear targets, the couplings can be determined by a set of four linearly independent measurements. The famous SLAC  $D(e, e')X$  experiment<sup>63</sup>, in conjunction with atomic physics experiments enabled a model independent measurement of  $\bar{\alpha}$  and  $\bar{\gamma}$ .

### V.1 The Mainz Parity Experiment

Recently, an experiment at Mainz<sup>64</sup> was completed that measured at backward electron scattering angles, emphasising a different combination of the coupling constants which allowed extraction of the combination  $\bar{\beta} + 0.04\bar{\delta} = 0.005 \pm 0.17$ . This result is displayed in Figure V.2 in the terms of the quark coupling constants  $C_{2d} = (-\bar{\beta} + \bar{\delta})$  and  $C_{2u} = (\bar{\beta} + \bar{\delta})$ , where the results of the SLAC experiment and of neutrino hadron scattering experiments are shown as well. Although a factor of three improvement compared to the previous state of affairs has been achieved in the axial vector coupling sector, the result still allows for a vanishing axial vector interaction ( $\bar{\beta} = \bar{\delta} = 0$ ). Using results of the previous experiments  $\bar{\beta}$  and  $\bar{\delta}$  could be separated, and their respective values determined to

$$\bar{\beta} = -0.04 \pm 0.19, \quad \bar{\delta} = 1.07 \pm 1.83.$$

Assuming the validity of the Standard Model the coupling constants are related to the weak mixing angle  $\theta_W$  in the following way:

$$\bar{\alpha} = -(1 - \sin^2\theta_W), \quad \bar{\beta} = -(1 - 4\sin^2\theta_W), \quad \bar{\gamma} = \frac{2}{3}\sin^2\theta_W, \quad \bar{\delta} = 0$$

With  $\sin^2\theta_W = 0.232 \pm 0.004$  it is obvious that the result of the Mainz experiments is in agreement with this value. However, the precision of the experiment is not sufficient to have impact on the determination of  $\sin^2\theta_W$ .

### V.2 The MIT-Bates Parity Experiment

Another experiment to measure parity violation in  $^{12}C(\bar{e}, e')^{12}C$  has recently been completed at MIT-Bates<sup>65</sup>. This experiment measured directly  $\bar{\gamma}$ , the isoscalar piece of the vector coupling with the result

$$\bar{\gamma} = 0.136 \pm 0.032 \pm 0.009,$$

which is in agreement with the prediction of the Standard Model of  $\bar{\gamma}_{SM} = 0.155$ .

It appears the most important outcome of both experiments is the demonstration that polarized electron scattering experiments allow control of systematic errors much below the  $10^{-7}$  level.

### V.3 The SAMPLE Experiment at MIT-Bates

A new experiment<sup>65,66</sup> has been approved for MIT-Bates to measure parity violation in elastic electron-proton scattering at backward angles. In this case the asymmetry depends on the elastic electromagnetic formfactors  $F_1^\gamma$ ,  $F_2^\gamma$ , and the neutral weak formfactors  $F_1^Z$ ,  $F_2^Z$ . The latter one is related to the proton anomalous moment coupling to the neutral weak current. In the Standard Model, and invoking strong isospin symmetry,  $F_2^Z$  can be related to the electromagnetic formfactors like

$$F_2^Z = \left(\frac{1}{2} - \sin^2\theta_W\right)F_2^\gamma - \frac{1}{4}F_2^e \quad ,$$

where  $F_2^e$  is a singlet piece which arises from equal contributions of all three quark flavors. Since it contains contributions from strange quarks it is sensitive to the possible presence of large  $s\bar{s}$  contributions to the proton structure<sup>67</sup>. Large  $s\bar{s}$  contributions have been suggested from two sources. Firstly, the analysis<sup>68</sup> of the pion-nucleon sigma term ( $\Sigma_{\pi N}$ ) suggests a 30%  $s\bar{s}$  contribution to the proton rest mass. Secondly, the spin-dependent structure functions of the proton, measured by the EMC collaboration have been interpreted<sup>69</sup> to indicate that the strange sea is polarised opposite to the nucleon spin. The parity violating asymmetry in elastic ep scattering is given by:

$$-\frac{G_F Q^2}{\sqrt{2}\pi\alpha\xi} [2\tau t g^2 \frac{\xi}{2} (F_1^\gamma + F_2^\gamma)(F_1^Z + F_2^Z) + (F_1^\gamma F_1^Z + \tau F_2^\gamma F_2^Z) - \frac{(E+E')}{2M_N} t g^2 \frac{\xi}{2} (1 - 4\sin^2\theta_W) G_1 (F_1^\gamma + F_2^\gamma)],$$

where  $\xi = F_1^{\gamma^2} + \tau F_2^{\gamma^2} + 2\tau t g^2 \frac{\xi}{2} (F_1^\gamma + F_2^\gamma)^2$ . At large electron scattering angles the first term dominates. The term with  $G_1$  is suppressed since  $(1 - 4\sin^2\theta_W)$  is small. Since  $F_1^Z \ll F_2^Z$  the asymmetry is essentially proportional to  $F_2^Z$ , and the term of interest  $F_2^e$  can immediately be extracted.

## VI. CONCLUSIONS/OUTLOOK

Measurements of polarization observables in photoabsorption and in electron scattering processes has already generated information relevant for understanding the structure of the nucleon and deuteron. Interest in polarization aspects of intermediate energy physics has sharply risen in recent years as the physics possibilities have become more clearly visible. The experimental tools (polarised gas and solid state targets, proton and neutron recoil polarimeters, and polarised electron sources), which are necessary to exploit these possibilities are under continued development. Their most efficient exploitation will be possible at the new DC electron machines which are now under construction. In conjunction with the use of large acceptance detectors and high precision magnetic spectrometers these instruments will help generate data which are essential for the study of fundamental properties of nucleons and nuclei.

## REFERENCES.

- <sup>1</sup> S. Brodsky and G. Farrar, Phys. Rev. Lett. 31, 1153 (1973), Phys. Rev. D11, 1309 (1975)  
Y. Matveev, R. Muradyan, and A. Tavkhelidze, Nuovo Cimento Let. 7, 719 (1973).
- <sup>2</sup> S. Galster et al., Nucl. Phys. B32, 221 (1971).
- <sup>3</sup> S. Platchkov et al., Nucl. Phys. A510, 740 (1990).
- <sup>4</sup> R.G. Arnold et al., Phys. Rev. Lett. 57, 174 (1986)
- <sup>5</sup> M. Gari, N. Stefanis, Phys. Lett. B187, 401 (1987)
- <sup>6</sup> N. Dombey, Rev. Mod. Phys. 41, 236 (1969)
- <sup>7</sup> R. Arnold, C. Carlson, F. Gross, Phys. Rev. C23, 363 (1981)
- <sup>8</sup> R. Holt, S. Popov, private communications (1990)
- <sup>9</sup> R. Milner, invited contribution, presented at this conference .
- <sup>10</sup> V.D. Burkert, Lecture Notes in Physics 234, 228(1984)
- <sup>11</sup> T. Reichelt, private communication (1990)
- <sup>12</sup> D. Day, private communication (1990)
- <sup>13</sup> A.K. Thompson et al., contributed paper 18C to this conference.
- <sup>14</sup> E.W. Otten, Lecture presented at the Erice Summer School (1989).
- <sup>15</sup> H. Arenhovel, W. Leidemann, and E.L. Tomusiak, Z. Phys. A331, 123 (1988)

- 16 M.P. Rehalo, G.I. Gakh, and A.P. Rehalo, J. Phys. G: Nucl. Part. 15, 1223 (1989).
- 17 B. Blankleider and R.M. Woloshyn, Phys. Rev. C29, 538 (1984);  
U. Meissner, Phys. Rev. Lett. 62, 1013 (1989).
- 18 C. Perdrisat, private communications; see also: V. Punjabi et al, contributed paper 10C.
- 19 V. Burkert, Proc. Workshop on Electronuclear Physics with Internal Beams and Targets, SLAC,(1987)
- 20 D. Crabb, University of Michigan Preprint, UM HE 89-31 (1989)
- 21 W. Warns, et al.; Z.Phys.C (1990)
- 22 C.E. Carlson, J.L. Poor, Phys. Rev. D38, 2758 (1988)
- 23 N. Isgur and G. Karl, Phys. Lett. 72B, 109 (1977); Phys. Rev. D23, 817 (1981)
- 24 I. Koniuk and N. Isgur, Phys. Rev. D31, 1868 (1980)
- 25 C.E. Carlson, Phys. Rev. D34, 3704 (1986)
- 26 R. Lourie (Spokesperson), Bates Proposal 89-03, C. Papanicolas (Spokesperson), Bates Proposal 87-09
- 27 V. Burkert (Spokesperson), CEBAF Proposals PR-89-37, PR-89-42
- 28 G. Kroesen and B. Boden, Research Program at CEBAF, Report of the Summer Study Group, Newport News, 1986.
- 29 F.E. Close, Proc. CEBAF Summer Workshop, Newport News, 1988.
- 30 R.W. Lourie, paper submitted to Phys. Rev. D, (1990).
- 31 L.S. Barker, A. Donnachie, and J.K. Storrow, Nucl. Phys. B95, 347 (1975)
- 32 R. Avakian et al., H.H. Vartapetian, private communications (1990)
- 33 F.V. Adamian et al., J.Phys.G: Nuclear Part. 14 (1988)
- 34 G. Anton, private communications
- 35 T. Barnes, F. Close, Phys. Letts. 123B, 89 (1983);  
E. Golovitch, E. Haqq, and G. Karl, Phys. Rev. D28, 160 (1983)
- 36 R.A. Adelbeck and B. Saghai, Rapport DPh-N/Saclay 2544B (1989).
- 37 S. Matone, invited contribution at this conference, parallel session C.
- 38 S.D. Drell and A.C. Hearn, Phys. Rev. Lett. 16, 908 (1966)
- 39 S. Gerasimov, Sov. J. Nucl. Phys. 3, 930 (1966)
- 40 I. Karliner, Phys. Rev. D7, 3717 (1973)
- 41 M.E. Schulse et al., Phys. Rev. Lett. 52, 597 (1984)
- 42 J. Cameron, private communications; see also Ref. 73.
- 43 R. Gilman et al., submitted to Phys. Rev. Lett. (1990)
- 44 R. Holt, invited talk presented at this conference.
- 45 B. Boden et al., Preprint BONN-ME-90-06 (1990)
- 46 C.E. Carlson, Nucl. Phys. A508, 481c (1990)
- 47 T. Kamae et al., Phys.Rev.Lett.38,468(1977)
- 48 A.A. Zyalov, et al., Yad. Fis.51, 32(1990)
- 49 W. Leidemann, H. Arenhovel, Nucl.Phys.A465,573(1987)
- 50 H. Tanabe and K. Ohta, Phys.Rev.C40,1905 (1989)
- 51 K.H. Althoff et al., Z.Phys.C43,375(1989)
- 52 R. Avakian et al. (1990), contribution by H. Vartapetian, parallel session C.
- 53 M. Laget, private communication, presented in Ref.49
- 54 J. Napolitano et al., Phys.Rev.Lett.61, 2530(1988)
- 55 T.S. Lee, Argonne National Laboratory, Physics Division, Report PHY-5253-TH-88.
- 56 C.E. Carlson, private communication (1990)
- 57 A.S. Bratashvskij et al., JETP Lett. 31, 370 (1980); JETP Lett. 34, 389 (1981); JETP Lett. 36, 216 (1982)
- 58 S. Turck-Chiese et al., Phys. Lett. 142B, 145 (1984)
- 59 H. Breuer et al., Nucl. Phys. A455, 641 (1986)
- 60 Y. Mel'nik, A.V. Shebeko, contributed papers 15C and 16C.
- 61 F.V. Adamian, et al., Phys.Lett.B232,296(1989)
- 62 V.B. Ganenko, V.A. Gushin et al., private communications by P.V. Sorokin (1990).
- 63 C.Y. Prescott et al; PL 77B, 347 (1978); PL 84B, 524 (1979)
- 64 W. Heil et al; Nucl. Phys. B327, 1 (1989)
- 65 S. Kowalski, invited talk presented at this conference
- 66 E. Beise et al., Bates Proposal 89-06 (1989)
- 67 D. Kaplan and A. Monahan, Nucl.Phys.B310,527 (1988)
- 68 R.L. Jaffe and C.L. Korpa, Comments Nucl. Part. Phys. 17, 103 (1987)
- 69 see the discussion by R.L. Jaffe, invited talk at this conferences
- 70 R. Madey, private communications (1990)
- 71 W.J. Metcalf and R.L. Walker, Nucl. Phys. B76, 253 (1974)
- 72 M. Garcon, invited talk presented at this conference